Available online at www.sciencedirect.com
SCIENCE DIRECT®
Computers and Geotechnics 31 (2004) 23–36
COMPUTERS AND GEOTECHNICS
www.elsevier.com/locate/compgeo

Lower bound solutions for bearing capacity of jointed rock

D.J. Sutcliffe [a], H.S. Yu [b,*], S.W. Sloan [c]

[a] Department of Civil, Surveying and Environmental Engineering, The University of Newcastle, NSW 2308, Australia
[b] Nottingham Centre for Geomechanics, The University of Nottingham, University Park, Nottingham NG7 2RD, UK
[c] Department of Civil, Surveying and Environmental Engineering, The University of Newcastle, NSW 2308, Australia

Received 15 July 2003; received in revised form 31 October 2003; accepted 11 November 2003

Abstract

This paper applies numerical limit analysis to evaluate the bearing capacity of strip footings on an anisotropic, homogenous material. While solutions exist for footings on jointed rock [Proceedings of the Third International Conference on Computational Plasticity 2 (1992) 935; Proceedings of the International Conference on Structural Foundations on Rock 3 (1980) 83] little work has been done on the effect of variation of joint strength and relative joint orientation (for cases with two or more joint sets). From a macroscopic point of view, many jointed materials such as rock may be assumed to have anisotropic homogenous properties. The overall behaviour of a jointed rock mass is controlled by the mechanical properties of the intact rock as well as the strength and orientation of the discontinuities. The formulation presented here assumes plane strain conditions, and makes use of the Mohr–Coulomb failure criterion.

In order to utilise the lower bound theorem of classical plasticity two basic assumptions must be made. Firstly the material is assumed to exhibit perfect plasticity and obey an associated flow rule without strain hardening or softening. Secondly, it is assumed that the body undergoes only small deformations at the limit load so that the effect of geometry changes is small.

By using a Mohr–Coulomb approximation of the yield surfaces, the proposed numerical procedure computes a statically admissible stress field via linear programming and finite elements. The stress field is modelled using linear three-noded triangular elements and allows statically admissible stress discontinuities at the edges of each triangle. By imposing equilibrium, yield and stress boundary conditions on the unknown stresses, an expression of the collapse load is formed which can be maximized subject to a number of linear constraints on the nodal stresses. As all the requirements are met for a statically admissible stress field, the solution obtained is a rigorous lower bound on the actual collapse load.

An extensive parametric analysis is presented to investigate the effects of joint orientation and strength properties on the overall bearing capacity of jointed rock. The analysis overcomes the limitations of previous solutions in that non-orthogonal joint sets are considered. Consequently this work represents an invaluable tool for designers.

Keywords: Anisotropic; Homogenous; Lower bound; Limit analysis; Bearing capacity

1. Introduction

Discontinuities in rock masses often display a strength less than that of the intact material. As such the presence of these joints creates planes of weakness along which failures may initiate and propagate. If the joint sets are reasonably constant in orientation, closely spaced and continuous, the overall behaviour of the rock mass may be assumed to be homogenous but anisotropic. The overall behaviour of the rock mass is then controlled by the mechanical properties of the intact rock as well as the strength and orientation of the discontinuities. Davis [4] presented a series of slip line solutions for the bearing capacity of footings on jointed rock. However, they are primarily concerned with a rock mass containing one or two orthogonal and similar joint sets. It should be noted that slip-line solutions give neither rigorous lower bound nor rigorous upper bound solutions on the actual collapse load [3].

* Corresponding author. Tel.: +44-115-84-66884; fax: +44-115-9513898.
E-mail address: hai-sui.yu@nottingham.ac.uk (H.S. Yu).

0266-352X/$ - see front matter © 2003 Elsevier Ltd. All rights reserved.
doi:10.1016/j.compgeo.2003.11.001

The finite element method has been used to model the collapse behavior of footings on jointed rock [1]. Despite being general, the displacement finite element method tends to over predict the true collapse load due to excessive kinematic constraints imposed by plastic flow rules (see [8,9]).

An alternative to the conventional finite element method for determining the collapse load of a footing on jointed rock is limit analysis using the lower bound theorem. The lower bound theorem states that the collapse load obtained from any statically admissible stress field will underestimate the true collapse load. A statically admissible stress field is one which (a) satisfies the equations of equilibrium, (b) satisfies the stress boundary conditions and (c) does not violate the yield criterion. Two basic assumptions must be made about the material in order to apply the lower bound theorem. Firstly, the material is assumed to be perfectly plastic, that is, the material exhibits ideal plasticity with an associated flow rule without strain hardening or softening. The level of ductility exhibited by a jointed rock mass is dependent on the imposed stress state. For example, a jointed rock material will display brittle failure under direct tension. On the other hand, under normal compression and/or shear force the material will exhibit significant ductility due to the sliding failure mode which occurs within the joints. Secondly, it is assumed that all deformations or changes in the geometry of the rock mass at the limit load are small and therefore negligible.

It is recognised that the lower bound theorem has been applied less frequently than the upper bound theorem as it is easier to construct a kinematically admissible failure mechanism than it is to construct a statically admissible stress field. Furthermore, the lower bound theorem is often difficult to apply to problems involving complex loading and geometry, particularly if it is necessary to construct the stress fields manually. In practice, a lower bound solution is more valuable as it results in a safe design.

The numerical approach, first presented by Lysmer [5] and later extended by Sloan [7], is used in the current paper to discretise the media into a collection of three-noded triangular stress elements with the nodal variables being the unknown stresses. Statically admissible stress discontinuities are allowed to occur at the interfaces between adjacent triangles. The application of the constraints of a statically admissible stress field leads to an expression for the collapse load which is maximized subject to a set of linear constraints.

The aim of this paper is firstly to present a general numerical method which can be used to calculate rigorous lower bound solution for jointed rock and, secondly, to apply this method to a parametric investigation of the problem of a rigid footing on a jointed rock mass. To achieve this, the conventional isotropic Mohr–Coulomb yield criterion has been generalised to account for the anisotropy caused by the presence of discontinuities. The numerical formulation of the lower bound limit theorem is then developed. In order to avoid the occurrence of non-linear constraints, a linear approximation of the yield criterion will be used. In doing so the application of the lower bound limit theorem leads to a linear programming problem. One major advantage of the finite element formulation of the lower bound theorem is the ease with which complex loading and boundary conditions, geometry and rock behaviour can be dealt with.

2. Problem definition

The plane strain bearing capacity problem to be considered is illustrated in Fig. 1. A strip of footing of width B rests upon a layer of jointed rock with intact strength properties c and ϕ, and joint strength properties c_i and ϕ_i, where $i = 1, \ldots,$ no. of joint sets.

The bearing capacity solution will be a function of the intact material strengths, and the strength and orientation of the joint sets.

3. Failure criterion for jointed rock material

3.1. Failure surface for the intact rock material

For the sake of simplicity it is assumed that the intact rock material is isotropic, homogenous and obeys the Mohr–Coulomb failure criterion. If tensile stresses are positive, the Mohr–Coulomb criterion for plane problems may be expressed as:

$$F_r = (\sigma_x - \sigma_y)^2 + (2\tau_{xy})^2 - (2c\cos\phi - (\sigma_x + \sigma_y)\sin\phi)^2 = 0, \quad (1)$$

where σ_x, σ_y are normal stresses in the horizontal and vertical directions, respectively, τ_{xy} is the shear stress,

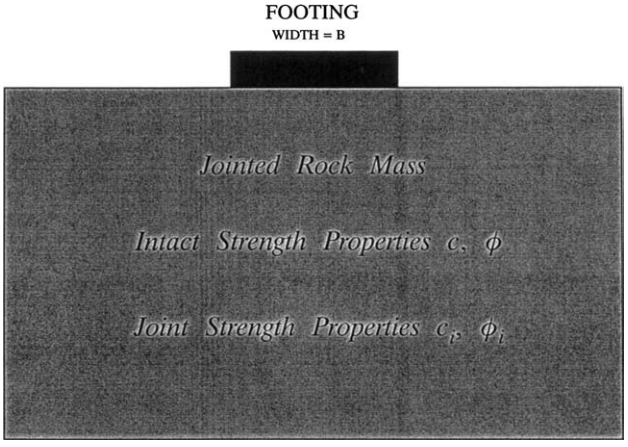

Fig. 1. Strip footing on a jointed rock.

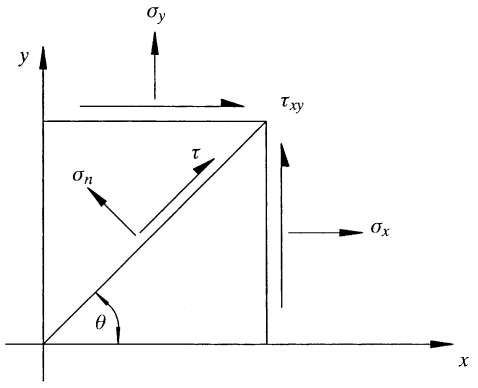

Fig. 2. Resolution of stresses into normal and shear components acting on a plane.

and c, ϕ denote the cohesion and friction angle of the intact rock material.

3.2. Failure surface for discontinuities

Following Davis [4], a cohesive-frictional Mohr–Coulomb failure criterion is also used to describe the limiting strength of the rock joints.

For any joint set i the linearised Mohr–Coulomb failure surface may be expressed as:

$$F_i = |\tau| - c_i + \sigma_i \tan\phi_i = 0, \tag{2}$$

where τ is the shear stress and σ_n is the normal stress on the joint. This failure criterion can be expressed in terms of σ_x, σ_y and τ_{xy} using the following relations:

$$\sigma_n = \sin^2\theta_i\sigma_x + \cos^2\theta_i\sigma_y - \sin 2\theta_i\tau_{xy}, \tag{3}$$

$$\tau = -\frac{1}{2}\sin 2\theta_i\sigma_x + \frac{1}{2}\sin 2\theta_i\sigma_y + \cos 2\theta_i\tau_{xy}, \tag{4}$$

where θ_i is the angle of the joint set i from the horizontal axis (positive anti-clockwise, refer Fig. 2).

Using the relations (3) and (4) the failure criterion expressed in (2) may be re-written as:

$$F_i = \frac{1}{2}|\sin 2\theta(\sigma_y - \sigma_x) + 2\cos 2\theta\tau_{xy}| - c_i + (\sin^2\theta\sigma_x + \cos^2\theta\sigma_y - \sin 2\theta\tau_{xy})\tan\phi_i = 0. \tag{5}$$

It should be noted that an identical failure criterion was derived by Bekaret and Maghous [2] for the more general case of non-orthogonal joints in three dimensions.

4. Finite element formulation of the lower bound theorem

According to the lower bound limit theorem, any statically admissible stress field will result in a lower bound estimate of the true collapse load. A statically admissible stress field is one which satisfies equilibrium and stress boundary conditions and does not violate the yield criterion.

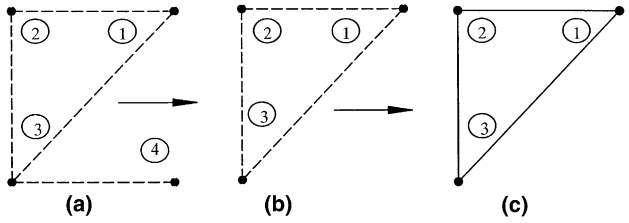

Fig. 3. Elements used in lower bound analyses. (a) Four-noded rectangular extension element, (b) three-noded triangular extension element and (c) three-noded triangular element.

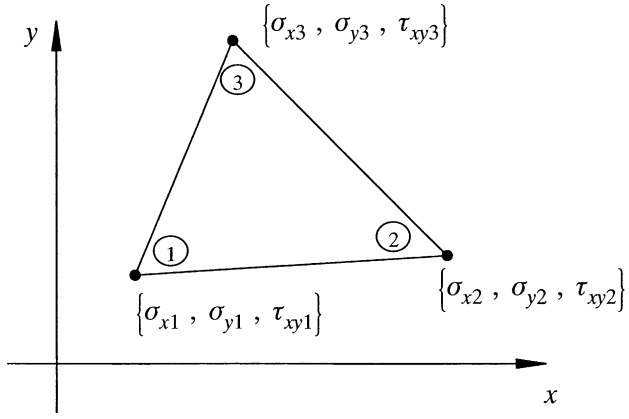

Fig. 4. Three-noded linear stress triangle with three unknown stresses at each node.

The finite element formulation of the lower bound theorem which follows uses three types of elements (Fig. 3) based on Sloan [7]. Each node is associated with three stresses, σ_x, σ_y, and τ_{xy} (Fig. 4) with the variation of stresses throughout each element assumed to be linear. The inclusion of triangular and rectangular extension elements extends the solution over a semi-infinite domain and therefore provides a complete statically admissible stress field.

Unlike the elements used in displacement finite element analysis, several nodes may share the same coordinate and each node is associated with only one element. In this way statically admissible stress discontinuities can occur at all edges between adjoining triangles. By ensuring the equations of equilibrium are satisfied, and that the stress boundary conditions and the yield criteria are not violated, a rigorous lower bound on the collapse load is obtained.

4.1. Element equilibrium

The stresses throughout each element must satisfy the following two equilibrium equations:

$$\frac{\partial \sigma_x}{\partial x} + \frac{\partial \tau_{xy}}{\partial y} = 0, \tag{6}$$

$$\frac{\partial \sigma_y}{\partial y} + \frac{\partial \tau_{xy}}{\partial x} = \gamma, \tag{7}$$

where tensile stresses are taken positive, a right handed Cartesian coordinate system is adopted and γ is the unit weight of the material. This results in two equality constraints on nodal stresses for each element.

4.2. Discontinuity equilibrium

It is necessary to impose additional constraints on the nodal stresses at the edges of adjacent triangles in order to permit admissible discontinuities. For a discontinuity to be statically admissible only the normal stress parallel to the discontinuity may be discontinuous, with continuity of the corresponding shear stresses and normal stresses perpendicular to the discontinuity maintained. With reference to Fig. 2, the normal and shear stresses acting on a plane inclined at angle θ to the x-axis (positive anti-clockwise) are given by Eqs. (3) and (4), respectively.

Looking at Fig. 5, for triangles a and b, equilibrium along the discontinuity (or common side) requires that at every point along this side:

$$\sigma_{\mathrm{n}}^a = \sigma_{\mathrm{n}}^b; \quad \tau^a = \tau^b. \tag{8}$$

Since stresses are confined to varying linearly along any element edge, an equivalent condition is achieved by enforcing the constraints:

$$\sigma_{n1}^a = \sigma_{n2}^b; \quad \sigma_{n3}^a = \sigma_{\mathrm{n}4}^b; \quad \tau_1^a = \tau_2^b; \quad \tau_3^a = \tau_4^b. \tag{9}$$

As such, each statically admissible discontinuity along an element edge results in four equality constraints on the nodal stresses.

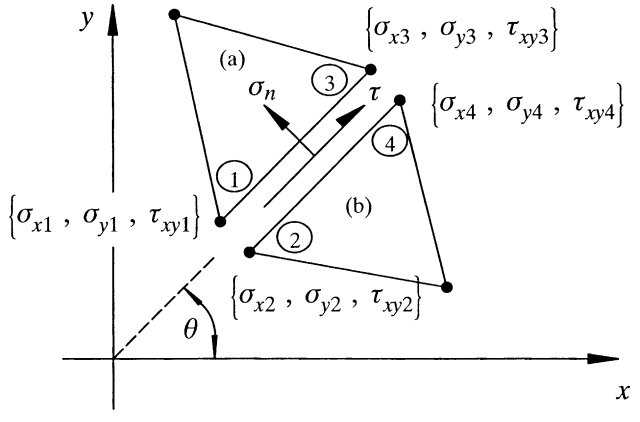

Fig. 5. Statically admissible stress discontinuity between adjacent triangles.

4.3. Boundary conditions

In order to enforce prescribed boundary conditions it is necessary to impose additional constraints on the nodal stresses. The problem of the bearing capacity of a footing has boundary conditions in the form of:

$$\sigma_{\mathrm{n}} = q = \text{constant}; \quad \tau = t = \text{constant}. \tag{10}$$

Given a linear variation of the stress components σ_x, σ_y and τ_{xy} along the edge of each triangle, a more general boundary condition may be imposed, in the form of (see Fig. 6):

$$\sigma_{\mathrm{n}}^l = q_1 + (q_2 - q_1)\xi; \quad \tau_{\mathrm{n}}^l = t_1 + (t_2 - t_1)\xi, \tag{11}$$

where l = edge of triangle e where boundary tractions are specified; ξ = local coordinate along l; q_1, q_2 = normal stresses specified at nodes 1 and 2 (tension positive); t_1, t_2 = shear stresses specified at nodes 1 and 2 (clockwise shears positive).

The boundary conditions of Eq. (17) are satisfied then by requiring

$$\sigma_{n1}^e = q_1; \quad \sigma_{n2}^e = q_2; \quad \tau_1^e = t_1, \quad \tau_2^e = t_2. \tag{12}$$

So for each edge where a boundary traction is specified, a maximum of four equality constraints on the nodal stresses are generated.

4.4. Yield condition

As described above, joints in the rock mass effectively modify the nature of the yield criterion. The effect of discontinuities is incorporated by including distinct failure surfaces for the intact rock material and for each of the joint sets. In this fashion the jointed rock mass is represented as a homogeneous but anisotropic material.

For the jointed rock material, the overall failure criterion is expressed by Eqs. (1) and (5). In order to satisfy the yield conditions it is necessary to impose the constraints $F_r \leqslant 0$ and $F_i \leqslant 0$. It is readily seen that for a joint set i the requirement that $F_i \leqslant 0$ results in two linear constraints on the nodal stresses. If however, the

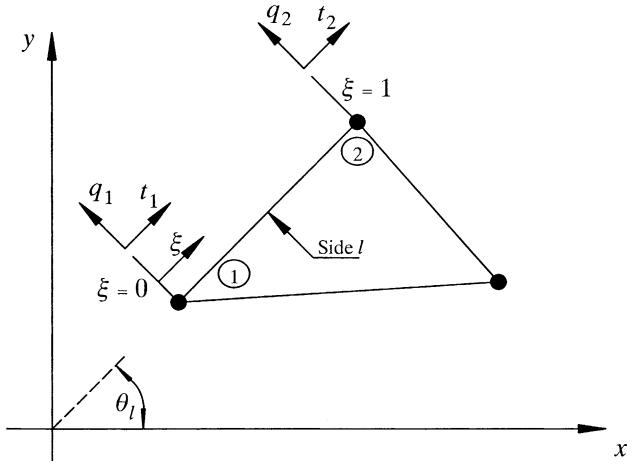

Fig. 6. Stress boundary conditions.

inequality constraints $F_r \leqslant 0$ is applied directly, non-linear constraints result since F_r is quadratic in the unknown stresses. Since the lower bound theorem is to be formulated as a linear programming problem, it is necessary to approximate (1) using a yield condition which is a linear function of the unknown stress variables. For the solution to be a rigorous lower bound the linear approximation to the failure surface must lie inside the generalized Mohr–Coulomb failure surface.

With reference to Fig. 7, if p is the number of sides used to approximate the yield function (1), then the linearised yield function can be shown to be [7]:

$$A_k\sigma_x + B_k\sigma_y + C_k\tau_{xy} \leqslant E, \quad k = 1, 2, \ldots, p, \tag{13}$$

where

$$A_k = \cos\left(\frac{2\pi k}{p}\right) + \sin\phi\cos\left(\frac{\pi}{p}\right),$$

$$B_k = -\cos\left(\frac{2\pi k}{p}\right) + \sin\phi\cos\left(\frac{\pi}{p}\right),$$

$$C_k = 2\sin\left(\frac{2\pi k}{p}\right),$$

$$E = 2c\cos\phi\cos\left(\frac{\pi}{p}\right).$$

Thus the linearised yield condition for the intact rock mass imposes p inequality constraints on the stresses at each node. In addition, the failure condition (5) for the joint leads to two linear inequality constraints on the unknown stresses:

$$A_k\sigma_x + B_k\sigma_y + C_k\tau_{xy} \leqslant c_i, \quad k = p + 2i - 1, \quad p + 2i, \tag{14}$$

where

$$A_{p+2i-1} = \sin^2\theta_i\tan\phi_i - \frac{1}{2}\sin 2\theta_i,$$

$$B_{p+2i-1} = \frac{1}{2}\sin 2\theta_i + \cos^2\theta_i\tan\phi_i,$$

$$C_{p+2i-1} = \cos 2\theta_i - \sin 2\theta_i\tan\phi_i,$$

$$A_{p+2i} = \sin^2\theta_i\tan\phi_i + \frac{1}{2}\sin 2\theta_i,$$

$$B_{p+2i} = -\frac{1}{2}\sin 2\theta_i + \cos^2\theta_i\tan\phi_i,$$

$$C_{p+2i} = -\cos 2\theta_i - \sin 2\theta_i\tan\phi_i.$$

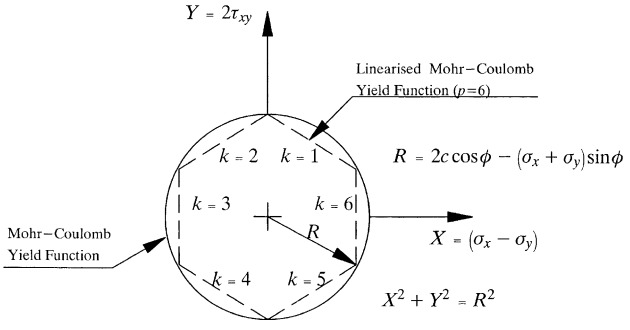

Fig. 7. Linearity Mohr–Coulomb yield function ($p = 6$).

By using a linearised failure surface it is sufficient to enforce the linear constraints (13) and (14) at each nodal point to ensure that the stresses satisfy the yield conditions everywhere.

4.5. Objective function

For many geotechnical problems, we seek a statically admissible stress field which maximises the integral of the normal stress over some part of the boundary. If the out-of-plane length of the footing is denoted by h, then the integral to be maximised is in the form of:

$$P = h\int_s \sigma_n \mathrm{d}s, \tag{15}$$

where P represents the collapse load. Due to the linear variation of stresses along any boundary it is possible to perform the integration analytically as:

$$P = \frac{h}{2}\sum_{\text{edges}}(\sigma_{n1} + \sigma_{n2})l_{12}, \tag{16}$$

where l_{12} is the length of the segment over which the force is to be optimized, defined by the nodes (1,2), and $(\sigma_{n1}, \sigma_{n2})$,$(\sigma_{x1}, \sigma_{x2})$, are the stresses at the segment ends.

4.6. Lower bound linear programming problem

By assembling the various constraints and objective functions the problem of finding a statically admissible stress field which maximises the collapse load may be written as:

$$\begin{aligned} &\text{Minimize} && -\boldsymbol{C}^T\boldsymbol{X}, \\ &\text{Subject to} && \boldsymbol{A}_1\boldsymbol{X} = \boldsymbol{B}_1, \\ & && \boldsymbol{A}_2\boldsymbol{X} \leqslant \boldsymbol{B}_2, \end{aligned} \tag{17}$$

where $\boldsymbol{A}_1$, $\boldsymbol{B}_1$ represent the coefficients due to equilibrium and stress boundary conditions; $\boldsymbol{A}_2$, $\boldsymbol{B}_2$ represent the coefficients for the yield conditions; $\boldsymbol{C}$ is the vector of objective function coefficients and $\boldsymbol{X}$ is the global vector of unknown stresses. An active set algorithm is used to solve the above linear programming problem, the details of which can be found in Sloan [7]. The solution for the unknown stresses $\boldsymbol{X}$ from (17) define a statically admissable stress field and, as such, the corresponding collapse load defines a rigorous lower bound on the true collapse load.

5. Numerical examples

To illustrate the effectiveness of the procedure described above, a number of examples will be analysed in this section. The results are compared with available solutions obtained from the literature.

5.1. Bearing capacity of a strip footing on rock with no joints

Prior to applying the finite element formulation of the lower bound limit theorem to jointed rocks, it is necessary to assess the accuracy of the numerical procedure. This is done by analysing a problem with a known closed form solution, for example, the problem of a strip footing on an intact rock material obeying the Mohr–Coulomb criterion.

The exact collapse pressure of a strip footing resting on a Mohr–Coulomb material with no overburden pressure is:

$$q = N_c c, \tag{18}$$

where $N_c = [\exp(\pi \tan\phi) \tan^2(\frac{\pi}{4} + \frac{\phi}{2}) - 1] \cot\phi$ and c is the cohesion. The mesh used to analyse the problem is shown in Fig. 8. For $\phi = 35°$, the exact value of N_c is 46.12 which compares well with the value of 41.02 obtained using the lower bound method with a p value of 24. If p is increased to 48, only a marginal improvement in accuracy is obtained, with an N_c value of 42.21. The corresponding increase in computational time is however over 300%. Fig. 9 shows the variation of q/c with friction angle using p values of both 24 and 48. It can be seen that strong agreement between the lower bound solution and the exact result is achieved for values of friction angle up to and including 35°. The variation between the true result and the lower bound solution at a friction angle of 0° is approximately 6.8%, increasing to a variation of 11.1% at a friction angle of 35° (see Fig. 9). Given the typical uncertainty of the material parameters, under prediction of the capacity of a footing by amounts of this order is considered to be sufficiently accurate, particularly since a conservative design is ensured.

It is important to note that the mesh shown in Fig. 8 includes extension elements, so the solutions obtained are valid throughout the infinite domain.

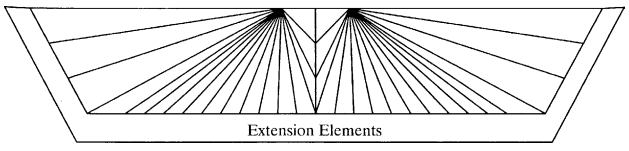

Fig. 8. Finite element mesh used for lower bound limit analysis of footing problem.

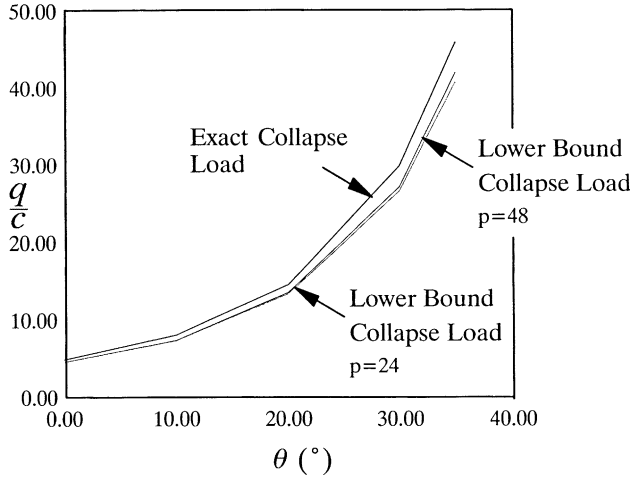

Fig. 9. Bearing capacity for a footing on an unjointed rock mass – comparison between lower bound and exact solution.

5.2. Bearing capacity of a strip footing on rock with one joint set

The problem of the bearing capacity of a rigid footing on a rock mass with one set of joints (Fig. 10) was also analysed. The mesh shown in Fig. 8 was again used. Ignoring the self weight of the material, the bearing capacity of the rock mass depends upon the cohesion and friction angle of the intact material and of the joint interfaces. Further, the orientation of the joint set plays a significant role in the determination of the collapse load.

Fig. 11 represents a comparison between the numerical lower bound solution and the displacement finite

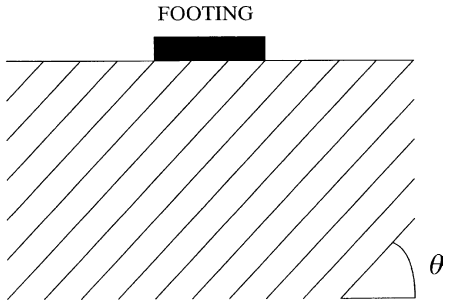

Fig. 10. Strip footing on a jointed rock mass with one joint set.

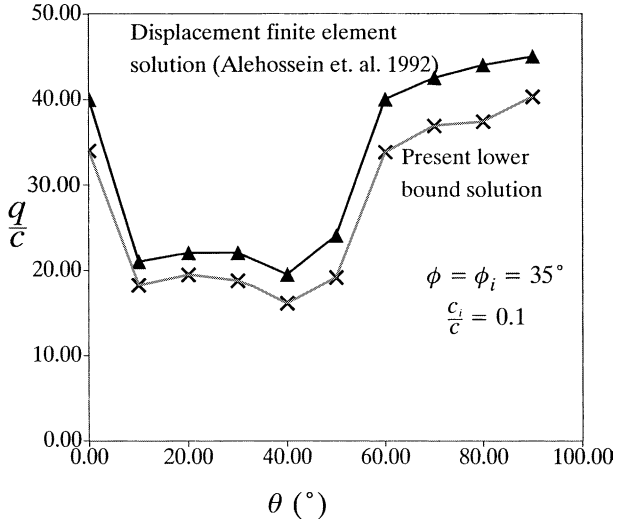

Fig. 11. Bearing capacity against joint set orientation – one joint set.

element solution of Alehossein et al. [1] for a perfectly smooth rock-footing interface. The results are presented as normalised bearing capacity against the orientation of the joint set and represent the solution for the case where $\phi = \phi_i = 35°$ and $c_i/c = 0.1$. As expected, the displacement finite element solutions of Alehossein et al. [1] tend to give higher results than those of the numerical lower bound method. The slip-line solution of Davis [4] also results in a slightly higher result due mainly to the fact that a slip-line solution is not necessarily a rigorous lower bound.

It should be noted from Fig. 11 that the minimum bearing capacity for this particular case occurs in the vicinity of joint orientations of 10° and 40° (note that the matrix of joint angle variations was $\Delta\theta_i = 10°$). The two minimum bearing capacities are approximately half the maximum bearing capacity which occurs when the joint set is aligned vertically.

Fig. 12 contains a comparison between the numerical lower bound solution and the upper bound solution of Maghous et al. [6] again for a rock mass with one joint set. The material properties used by Maghous et al. were $\phi = 30°$, $\phi_i = 20°$ and $c_i/c = 0.0$, 0.25, 0.5 for joint orientations of $\theta = 0$–45°. The results are presented as the ratio of the bearing capacity of the jointed rock mass to the bearing capacity of the intact rock mass vs. joint orientation (F_u/F_0 vs. θ). Similar to those comparisons discussed above, the lower bound solution leads to a more conservative result than the upper bound solution presented by Maghous et al. The general shape of the curves however is similar.

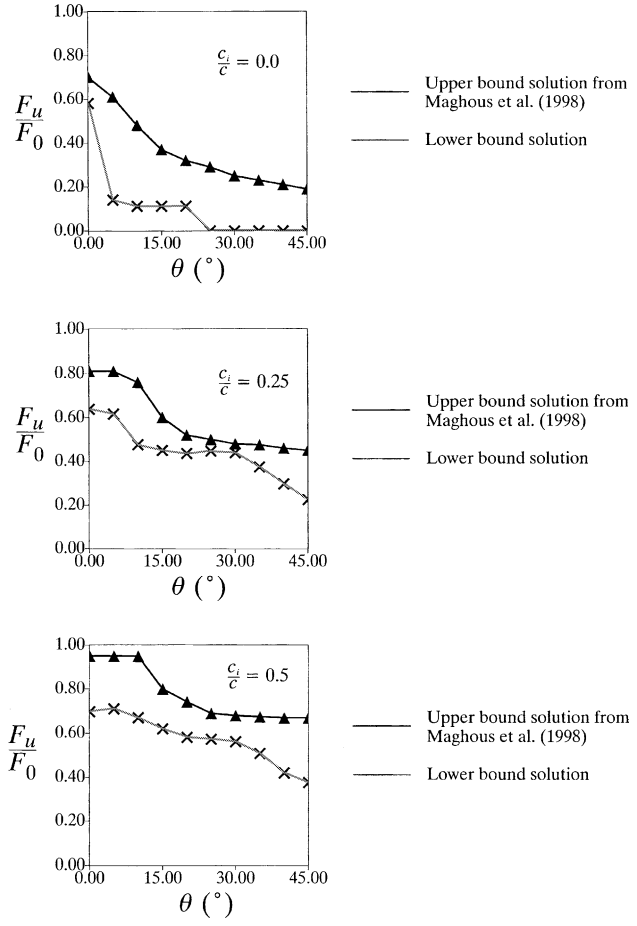

Fig. 12. Bearing capacity against joint set orientation – comparison between lower bound and upper bound solution of Maghous et al. [6].

Analyses were also carried out on the effect of variation of c_i/c and ϕ_i on the bearing capacity (Figs. 13 and 14). It can be seen that when $c_i/c = 0.1$ a reduction in strength in excess of 60% is possible, depending on the joint orientation. Similarly when the joint friction angle is reduced to 20°, a strength reduction of around 54% is experienced. As the value of cohesion and/or friction

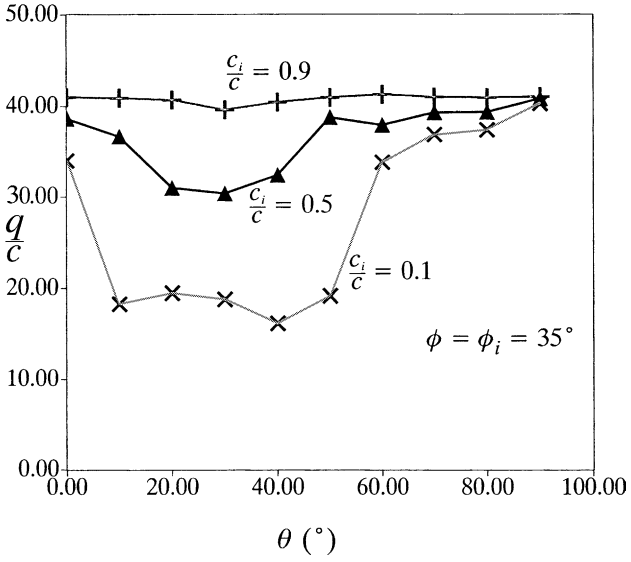

Fig. 13. Effect of c_i/c on bearing capacity – one joint set.

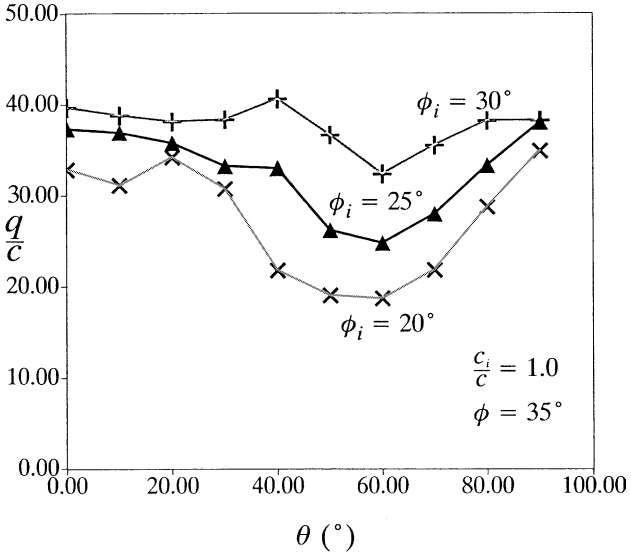

Fig. 14. Effect of ϕ_i on bearing capacity – one joint set.

angle on the joint set approaches the strength values of the intact material, the effect of the joint set on the overall bearing capacity of the material is significantly reduced. It is interesting to note that the effect of varying c_i/c is more pronounced for joint orientations in the range of 10° to 40°, while variation in ϕ_i results in a more pronounced effect in the joint orientation range of 40° to 70°.

5.3. Bearing capacity of a strip footing on rock with two joint sets

The third problem to be analysed is that of the bearing capacity of a strip footing on a rock mass with two joint sets as shown in Fig. 15. Fig. 16 shows the comparison between the normalised bearing capacity for current lower bound solution and the displacement finite element solution of Alehossein et al. [1] for the case where the joint sets are orthogonal and $\phi = \phi_i = 35°$, $c_i/c = 0.1$. As with the first example, the lower bound solution produces results less than that of the displacement finite element method. It can be seen that the minimum bearing capacities occurring the vicinity of joint orientations of 20°, 110° and 70°, 160° (note again the the matrix of joint angle variations was $\Delta\theta_i = 10°$). The maximum bearing capacity is achieved when the joint sets are orientated vertical and horizontal.

Once again analyses were performed on the effect of c_i/c and ϕ_i as well as the effect of relative joint orientation $d\theta$. Relative joint orientations of $d\theta = 90°, 75°, 60°, 45°, 30°, 15°$ were chosen with the results for $\phi = \phi_i = 35°$, $c_i/c = 0.1$, 0.5, 0.9 shown in Figs. 17–22 and results for $\phi = 35°$, $\phi_i = 20°$, 25°, 30° and $c_i/c = 1.0$ contained in Figs. 23–28.

Looking at Figs. 17–22, for the case of variation of joint cohesion and relative joint orientation a minimum bearing capacity in the order of 13% of the capacity of the intact rock mass occurred for $c_i/c = 0.1$ and

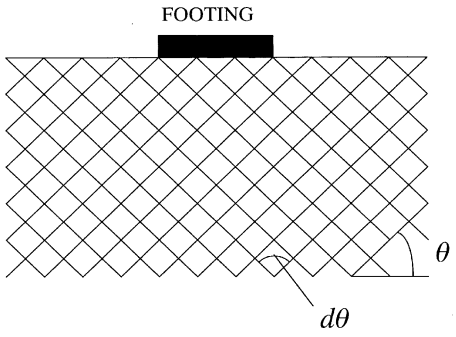

Fig. 15. Strip footing on a jointed rock mass with two joint sets.

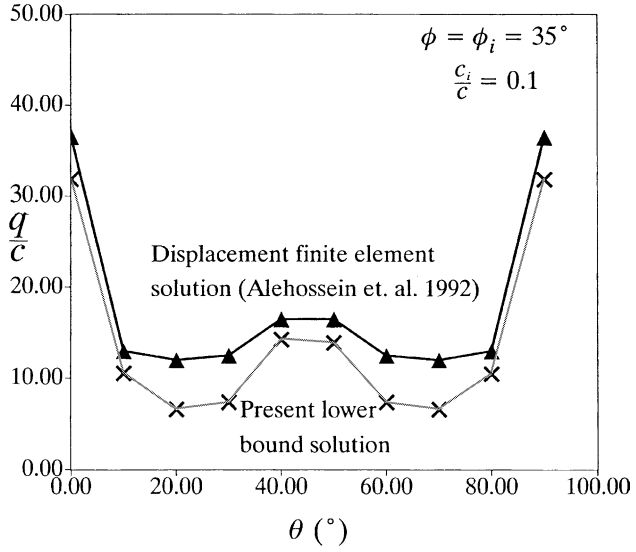

Fig. 16. Bearing capacity against joint set orientation – two orthogonal joint sets.

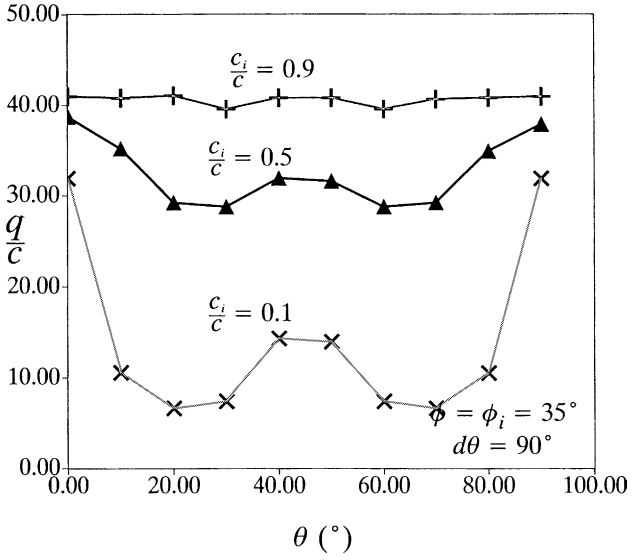

Fig. 17. Effect of c_i/c on bearing capacity – two joint sets – $d\theta = 90°$.

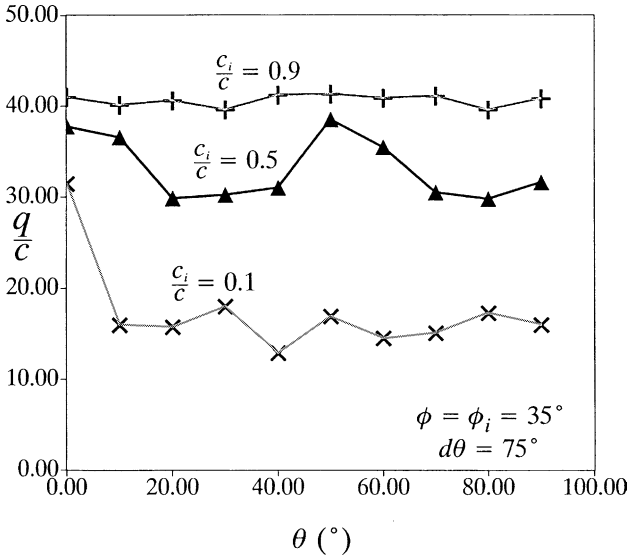

Fig. 18. Effect of c_i/c on bearing capacity – two joint sets – $d\theta = 75°$.

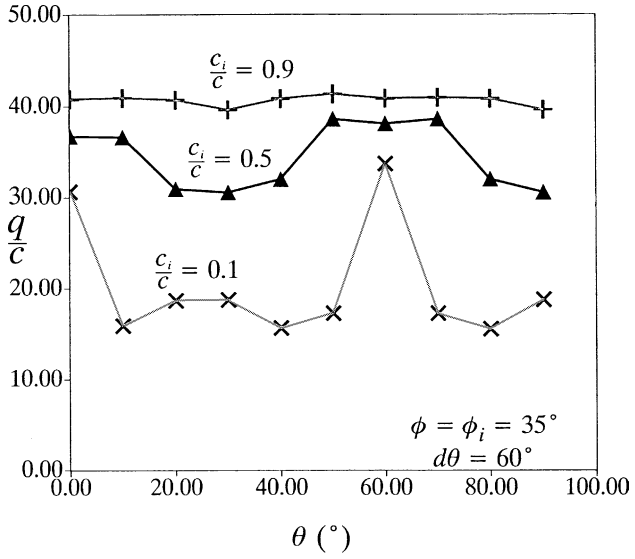

Fig. 19. Effect of c_i/c on bearing capacity – two joint sets – $d\theta = 60°$.

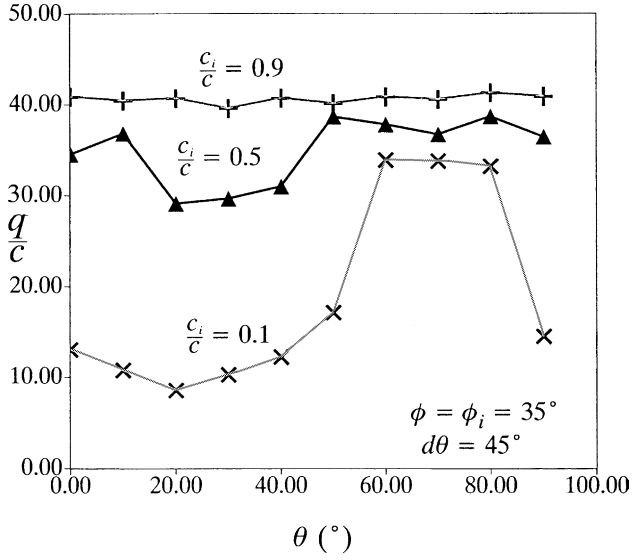

Fig. 20. Effect of c_i/c on bearing capacity – two joint sets – $d\theta = 45°$.

$d\theta = 30°$. A minimum bearing capacity of approximately 40% of the intact rock strength was achieved when $\phi_i = 20°$ for $d\theta = 30°$ and 45°. Again, as the values of joint strength (c_i, ϕ_i) approached the strength values of the intact material (c, ϕ), the bearing capacity of the joint rock mass approached that of the intact rock material.

It is interesting to observe the effect a variation of relative joint orientation has on the shape of the plots shown in Figs. 17–28. As expected, when the joint sets are orthogonal (Figs. 17 and 23), the plot of normalised bearing capacity vs. joint orientation is symmetric about $\theta = 45°$. However, where $d\theta = 15°$, the shape of the curve is very similar to that for a rock mass with a single joint set. (Compare Figs. 13 and 22 and Figs. 14 and 28).

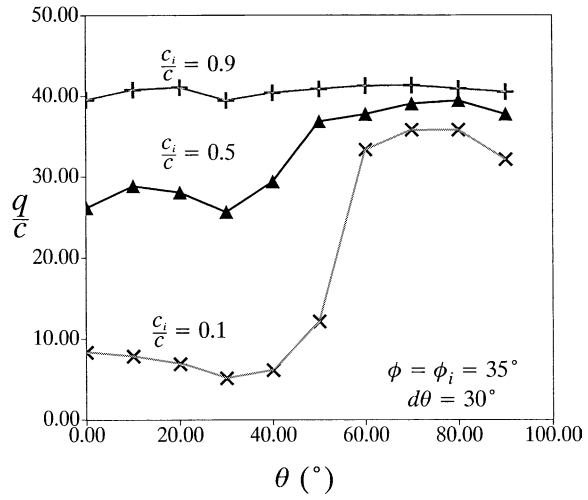

Fig. 21. Effect of c_i/c on bearing capacity – two joint sets – $d\theta = 30°$.

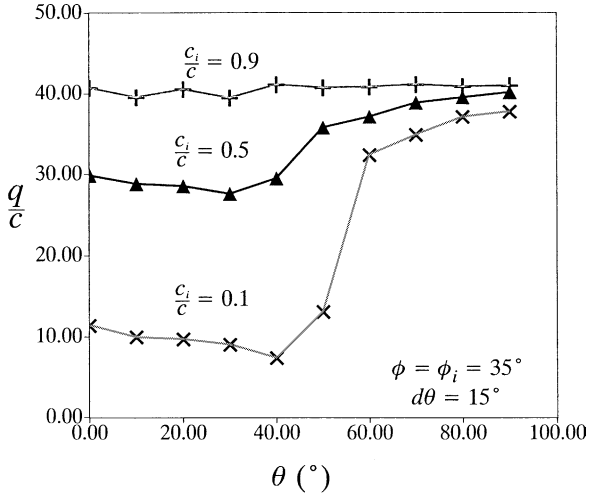

Fig. 22. Effect of c_i/c on bearing capacity – two joint sets – $d\theta = 15°$.

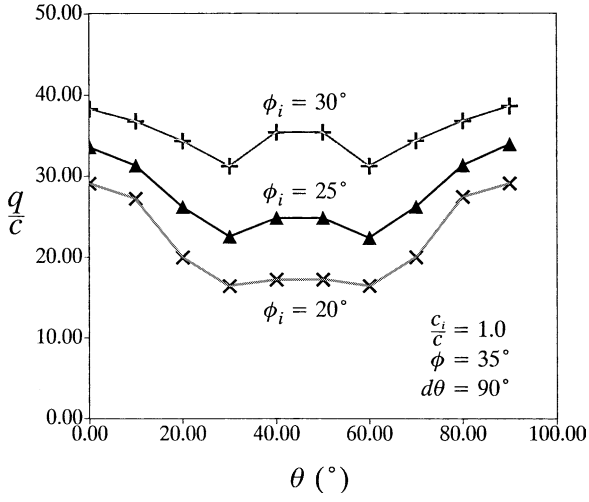

Fig. 23. Effect of ϕ_i on bearing capacity – two joint sets – $d\theta = 90°$.

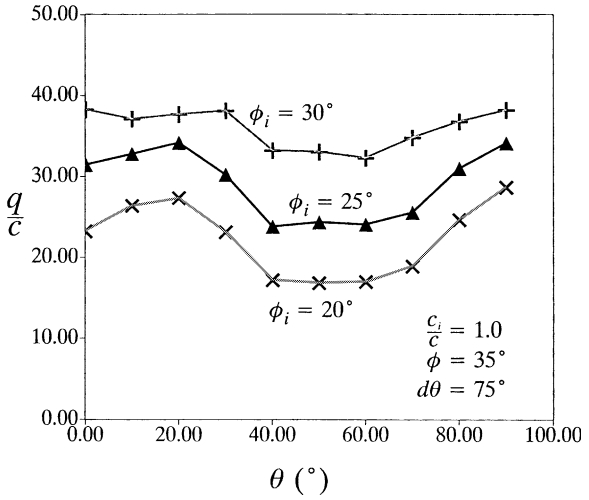

Fig. 24. Effect of ϕ_i on bearing capacity – two joint sets – $d\theta = 75°$.

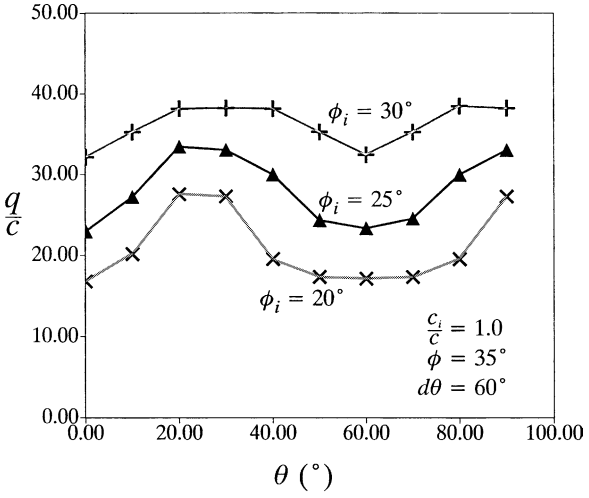

Fig. 25. Effect of ϕ_i on bearing capacity – two joint sets – $d\theta = 60°$.

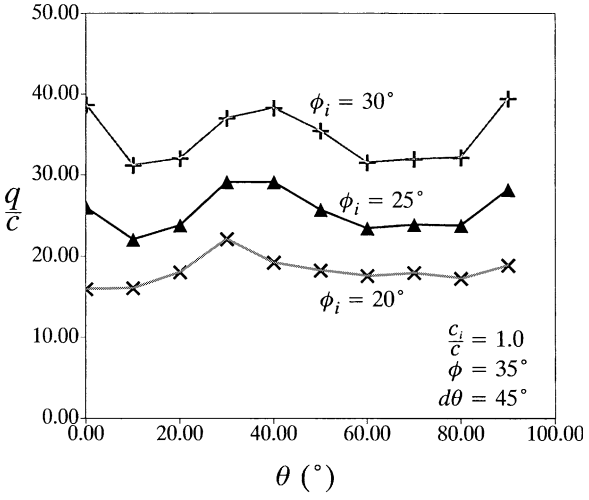

Fig. 26. Effect of ϕ_i on bearing capacity – two joint sets – $d\theta = 45°$.

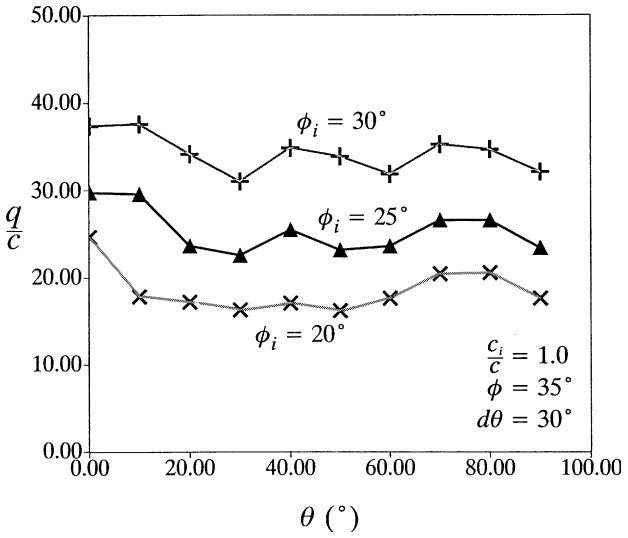

Fig. 27. Effect of ϕ_i on bearing capacity – two joint sets – $d\theta = 30°$.

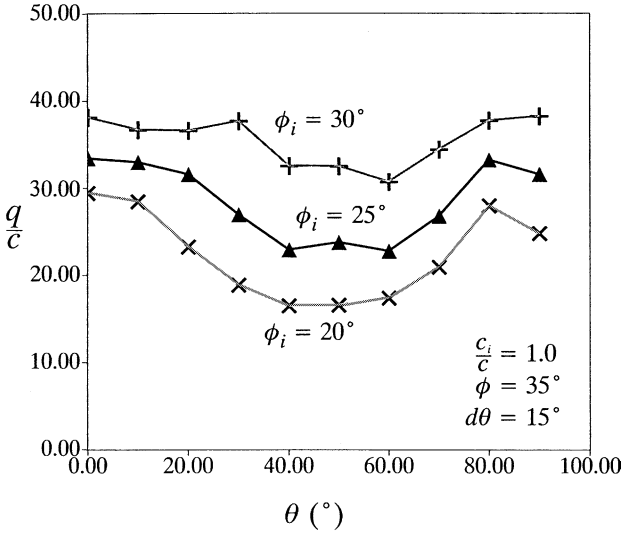

Fig. 28. Effect of ϕ_i on bearing capacity – two joint sets – $d\theta = 15°$.

One final result on the effect of variation of relative joint orientation should be noted for rock masses where $\phi = \phi_i$ and $c_i/c < 1.0$ (Figs. 17–22). With large values of $d\theta$ (say $d\theta = 90°$, 75°), the value of joint orientation (θ) is not particularly critical. That is, regardless of joint set orientation a significant reduction in bearing capacity can be expected. One exception is of course where the joint sets are orthogonal and aligned horizontally and vertically. For values of $d\theta$ less than 45° the value of joint orientation is a critical parameter with significant bearing capacity reduction only experienced for values of θ less than 50°. No such conclusion was drawn for the results for $c_i/c = 1.0$ (Figs. 23–28), where it would appear the value of $d\theta$ is always critical, regardless of joint orientation (θ).

5.4. Bearing capacity of a strip footing on rock with three joint sets

The final example is a simple extension of third example above. Analyses were performed on a strip footing on a jointed rock mass with two joints sets at varying orientations and a third joint set aligned vertically (Fig. 29). Unlike the previous examples there are no existing solutions for the bearing capacity of this problem.

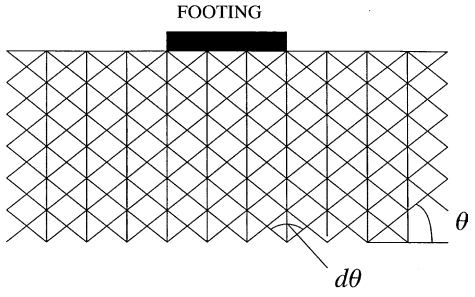

Fig. 29. Strip footing on a jointed rock mass with three joint sets.

Again variation of both θ and dθ are considered with results for $\phi = \phi_i = 35°$ and $c_i/c = 0.1$, 0.5, 0.9 shown in Figs. 30–35 and for $\phi_i = 20°$, 25°, 30° and $c_i/c = 1.0$ shown in Figs. 36–41. For reasons of comparison the results for a rock mass containing only two sets of joints are also shown (i.e. no vertical joint).

It is evident from these results that the inclusion of a third, vertically aligned joint set results in a further

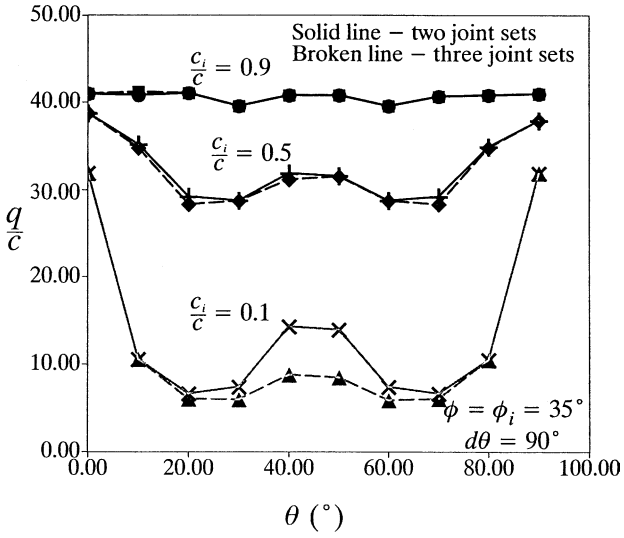

Fig. 30. Effect of c_i/c on bearing capacity – two and three joint sets – d$\theta = 90°$.

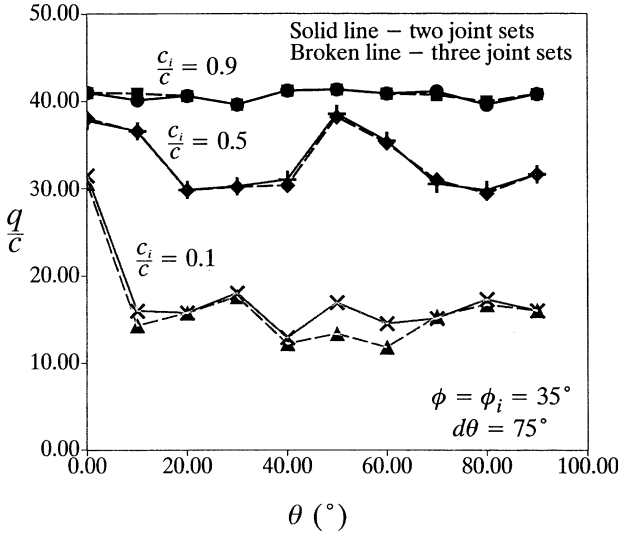

Fig. 31. Effect of c_i/c on bearing capacity – two and three joint sets – d$\theta = 75°$.

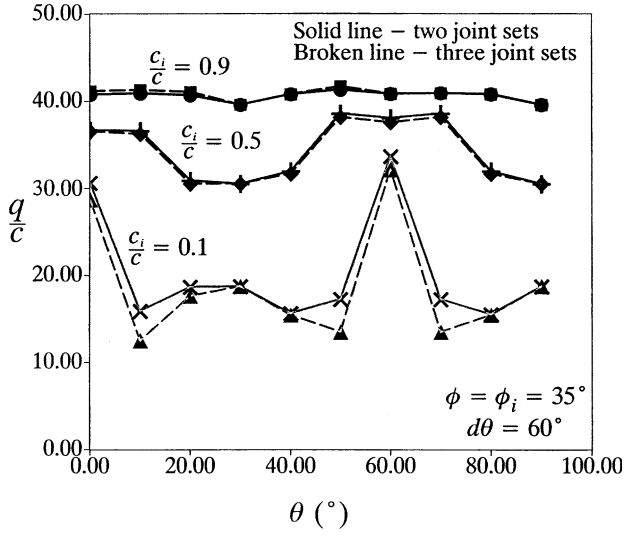

Fig. 32. Effect of c_i/c on bearing capacity – two and three joint sets – d$\theta = 60°$.

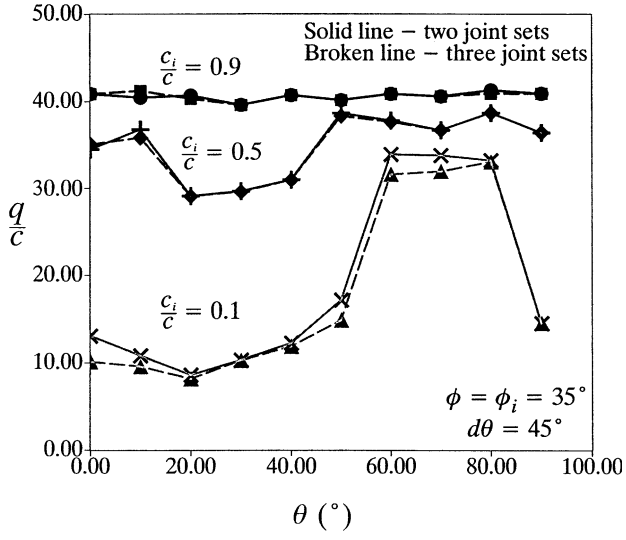

Fig. 33. Effect of c_i/c on bearing capacity – two and three joint sets – d$\theta = 45°$.

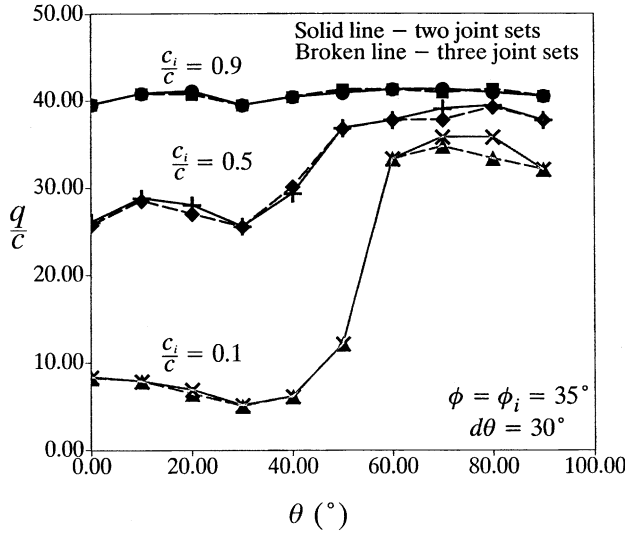

Fig. 34. Effect of c_i/c on bearing capacity – two and three joint sets – $d\theta = 30°$.

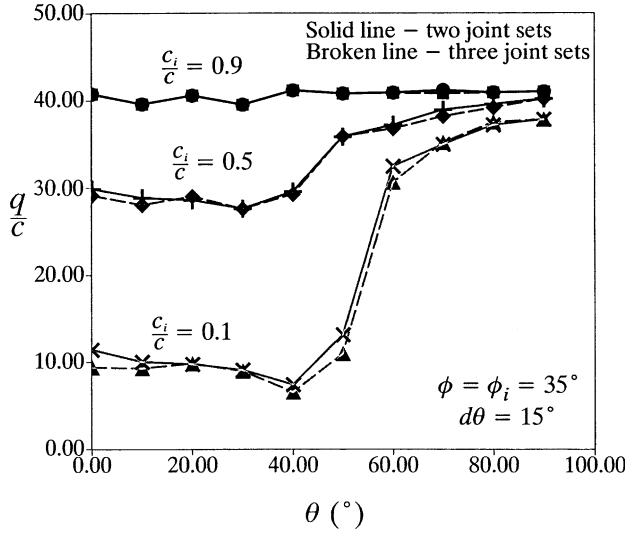

Fig. 35. Effect of c_i/c on bearing capacity – two and three joint sets – $d\theta = 15°$.

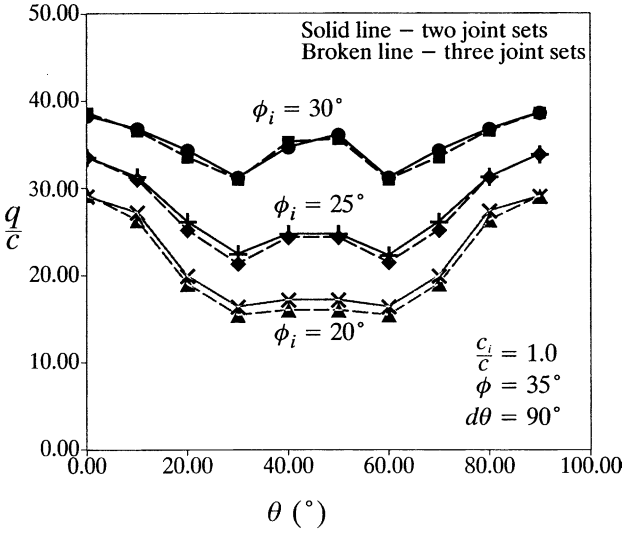

Fig. 36. Effect of ϕ_i on bearing capacity – two and three joint sets – $d\theta = 90°$.

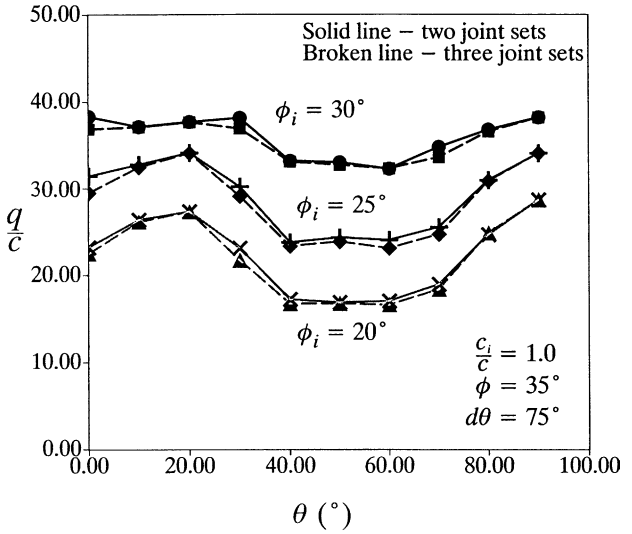

Fig. 37. Effect of ϕ_i on bearing capacity – two and three joint sets – $d\theta = 75°$.

reduction in overall bearing capacity. The value of this reduction in capacity is again dependant on both the joint orientation and the relative orientation between the joint sets. However loss of capacity up to 40% where $\phi = \phi_i = 35°$, $c_i/c = 0.1$ and up to 7% where $\phi_i = 20°$, $c_i/c = 1.0$ is experienced when compared to the solution for two joint sets only.

6. Conclusions

A rigorous finite element formulation of the lower bound theorem for a jointed rock mass has been presented. This technique assumes the jointed rock material can be treated as homogeneous and anisotropic. The formulation is capable of dealing with an arbitrary number of joint sets in the rock mass.

Using the technique presented, rigorous lower bound solutions for the ultimate bearing capacity of a surface footing resting on a jointed rock mass was investigated. Consideration was given to the effect of the number of joint sets present in the rock mass as well as variation of cohesive and frictional strength of these joint sets. Further, the effect of the joint sets orientation in relation to the horizontal, as well as the relative orientation of the joints (where two or more joint sets were present) was investigated. Results were presented in terms of

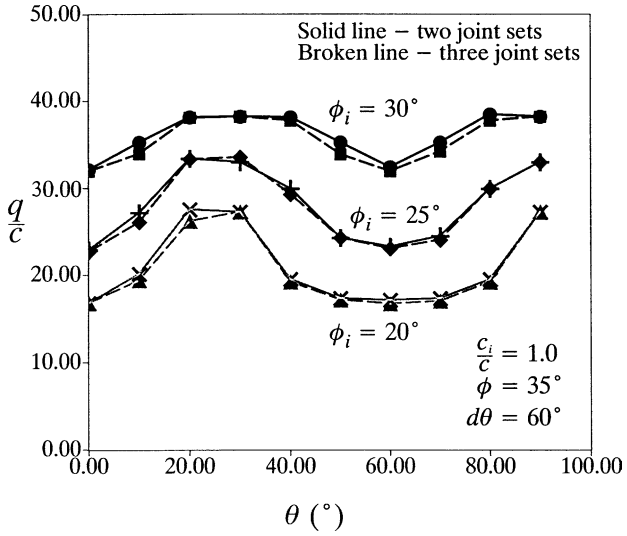

Fig. 38. Effect of ϕ_i on bearing capacity – two and three joint sets – $d\theta = 60°$.

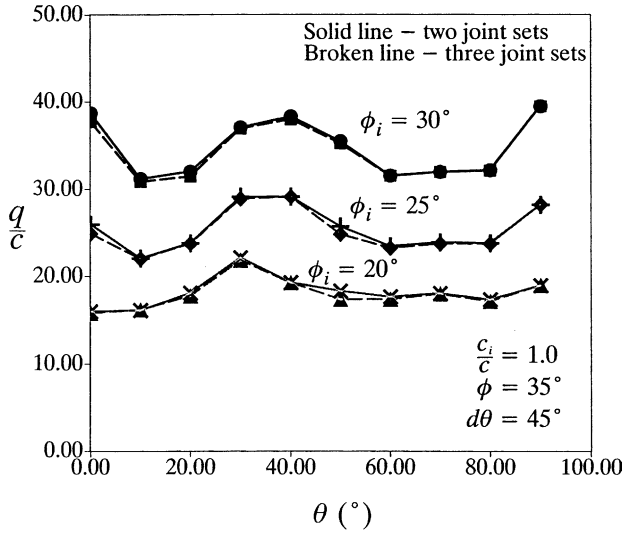

Fig. 39. Effect of ϕ_i on bearing capacity – two and three joint sets – $d\theta = 45°$.

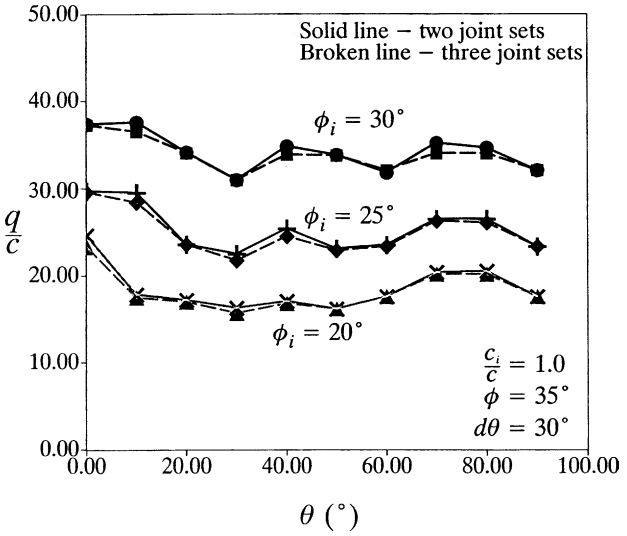

Fig. 40. Effect of ϕ_i on bearing capacity – two and three joint sets – $d\theta = 30°$.

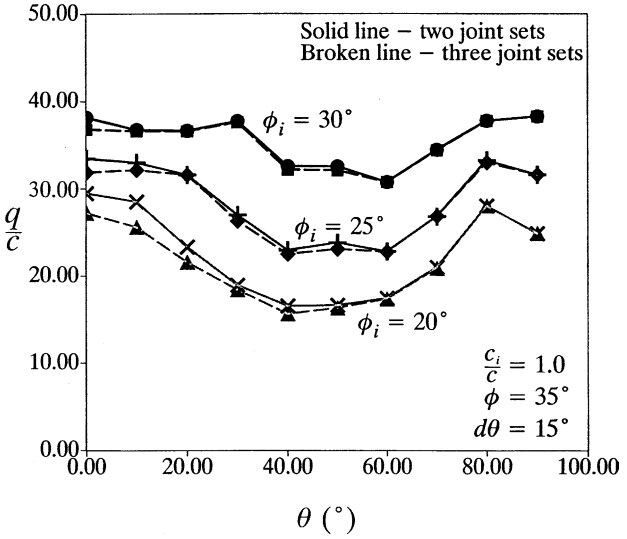

Fig. 41. Effect of ϕ_i on bearing capacity – two and three joint sets – $d\theta = 15°$.

normalised bearing capacity (q/c) against joint orientation.

The following conclusions can be made on the basis of the lower bound results presented:

- The lower bound solutions presented yield lower results than either the displacement finite element results of Alehossein et al. [1] or the slip-line results of Davis [4].
- Inclusion of a single weak joint set in a rock mass can reduce the bearing capacity by amounts in excess of 60%. However, the overall reduction in strength is significantly affected by both the strength of the joint relative to the properties of the intact rock material and to the orientation of the joint set.
- Where the rock mass has two joint sets present, the ultimate bearing capacity is further affected with possible reductions in capacity in the order of 87% (as compared to the result for an intact rock mass). Again the strength of the joints as well as the joint orientation significantly affects the result, although in this case the angle between the two joint sets also plays an important role.
- The inclusion of a third joint set vertically oriented results in a further loss in ultimate bearing capacity of up to 40% as compared to the results for a rock mass with two joint sets only. Parameters similar to those in the two joint case were again found to be critical.

Finally the parametric analysis presented in this paper is relevant to designers as it addresses the previously unexplored problem involving footings on a rock mass with non-orthogonal joint sets. Using the lower bound limit theorem not only extends previous work, it also ensures an inherently safe design.

References

[1] Alehossein H, Carter JP, Booker JR. Finite element analysis of rigid footings on jointed rock. Proceedings of the Third International Conference on Computational Plasticity, vol. 2, 1992. p. 935–45.

[2] Bekaret A, Maghous S. Three-dimensional yield strength properties of jointed rock mass as a homogenized medium. Mech Cohesive-Friction Mater 1996;1:1–24.

[3] Chen WF, Drucker DC. Bearing capacity of concrete blocks or rock. Journal of the Engineering Mechanics Division. Proceedings of the American Society of Civil Engineers 95(EM4) 1969. p. 955–79.

[4] Davis EH. A note on some plasticity solutions relevant to the bearing capacity of brittle and fissured materials. Proceedings of the International Conference on Structural Foundations on Rock, vol. 3, 1980. p. 83–90.

[5] Lysmer J. Limit analysis of plane problems in soil mechanics. Journal of the Soil Mechanics and Foundations Division, ASCE 1970;96:1311–34.

[6] Maghous S, de Buhan P, Bekaert A. Failure design of jointed rock structures by means of a homogenization approach. Mech Cohesive-Friction Mater 1998;3:207–28.

[7] Sloan SW. Lower bound limit analysis using finite elements and linear programming. Int J Anal Meth Geomech 1988;12:61–77.

[8] Sloan SW, Randolph MF. Numerical prediction of collapse load using finite elements and linear programming. Int J Anal Meth Geomech 1982;6:47–76.

[9] Yu HS, Houlsby GT, Burd HJ. A novel isoparametric finite element displacement formulation for axisymmetric analysis of nearly incompressible materials. Int J Numer Meth Eng 1993;36:2453–72.